Bioorganic & Medicinal Chemistry 19 (2011) 4739–4745

Contents lists available at ScienceDirect

Bioorganic & Medicinal Chemistry

journal homepage: www.elsevier.com/locate/bmc

Thermodynamic and biological evaluation of a thrombin binding aptamer modified with several unlocked nucleic acid (UNA) monomers and a 2′-*C*-piperazino-UNA monomer

Troels B. Jensen [a], Jonas R. Henriksen [b], Bjarne E. Rasmussen [c], Lars M. Rasmussen [c], Thomas L. Andresen [b], Jesper Wengel [a], Anna Pasternak [a,*]

[a] *Nucleic Acid Center, Department of Physics and Chemistry, University of Southern Denmark, Campusvej 55, 5230 Odense M, Denmark*
[b] *Department of Micro and Nanotechnology, Ørsteds Plads Building 345 East, DK-2800 Kgs. Lyngby, Denmark*
[c] *Department of Clinical Biochemistry and Pharmacology, Odense University Hospital, University of Southern Denmark, Sdr. Boulevard 29, 5000 Odense C, Denmark*

ARTICLE INFO

Article history:
Received 10 May 2011
Revised 27 June 2011
Accepted 30 June 2011
Available online 7 July 2011

Keywords:
Thrombin binding aptamer
Unlocked nucleic acid
Isothermal titration calorimetry
Thermodynamics
Thrombin time assay

ABSTRACT

Thrombin binding aptamer is a DNA 15-mer which forms a G-quadruplex structure and possess promising anticoagulant properties due to specific interactions with thrombin. Herein we present the influence of a single 2′-*C*-piperazino-UNA residue and UNA residues incorporated in several positions on thermodynamics, kinetics and biological properties of the aptamer. 2′-*C*-Piperazino-UNA is characterized by more efficient stabilization of quadruplex structure in comparison to regular UNA and increases thermodynamic stability of TBA by 0.28–0.44 kcal/mol in a position depending manner with retained quadruplex topology and molecularity. The presence of UNA-U in positions U3, U7, and U12 results in the highest stabilization of G-quadruplex structure ($\Delta\Delta G^{\circ}_{37}$ = −1.03 kcal/mol). On the contrary, the largest destabilization mounting to 1.79 kcal/mol was observed when UNA residues were placed in positions U7, G8, and U9. Kinetic studies indicate no strict correlation between thermodynamic stability of modified variants and their binding affinity to thrombin. Most of the studied variants bind thrombin, albeit with decreased affinity in reference to unmodified TBA. Thrombin time assay studies indicate three variants as being as potent as TBA in fibrin clotting inhibition.

1. Introduction

Thrombin is a serine protease involved in the blood coagulation cascade.[1] Inhibition of thrombin is applied in coronary surgery, prevention and treatment of cardiovascular diseases, and cancer therapy.[2–5] Development of novel thrombin inhibitors is of interest due to a number of side effects of anticoagulants used at present. Thrombin binding aptamer (TBA) is a short DNA sequence (5′GGTTGGTGTGGTTGG3′) which was found as a result of in vitro selection targeted towards thrombin.[6] This consensus 15-mer forms an intramolecular, antiparallel G-quadruplex structure with a chair-like conformation (Fig. 1).[7,8] The core constitutes of two G-quartets linked at one end by a TGT loop and by two TT loops at the other end. TBA is characterized by strong anticoagulant properties in vitro, short in vivo lifetime and rapid onset of action facilitating reversal of its activity and excluding dose-adjusting complications observed for other, commonly used anticoagulants.[9] Recently, TBA progressed through preclinical to clinical development (ARC183, Archemix).[10]

According to NMR and X-ray studies, TBA forms a complex with two thrombin molecules inactivating only one of them.[7,11,12] The inhibitory properties of TBA are attributed to specific interaction of the aptamer with the thrombin anion exosite I of one of the thrombin molecules. The electropositive heparin exosite of the second thrombin molecule is involved in neutralization of the nega-

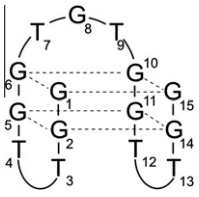

Figure 1. Quadruplex structure of thrombin binding aptamer (TBA).

Abbreviations: TBA, thrombin binding aptamer; UNA, unlocked nucleic acid; ITC, isothermal titration calorimetry; SPR, surface plasmon resonance; CD, circular dichroism; TDS, thermal difference spectra.

* Corresponding author. Tel.: +45 65502510; fax: +45 66158780.
E-mail address: apa@ifk.sdu.dk (A. Pasternak).

0968-0896/$ - see front matter © 2011 Elsevier Ltd. All rights reserved.
doi:10.1016/j.bmc.2011.06.087

tively charged backbone of the aptamer. It is still unresolved which part of the aptamer interacts with thrombin anion exosite I since X-ray studies indicate the middle TGT loop to be involved while NMR results suggest that interactions responsible for inhibitory process rather occur via the two TT loops.[7,11,12]

Unlocked nucleic acid (UNA) is an acyclic RNA mimic (Fig. 2a). The missing bond between the C2′ and C3′ atoms of the ribose ring results in increased flexibility relative to an RNA monomer. The UNA thymine monomer was first synthesized in 1995 and shown to significantly decrease thermal stability of DNA duplexes.[13] Recently, the synthesis of UNA-A, -C, -G, and -U phosphoramidites, introduction of all UNA monomers into RNA and DNA duplexes and thermodynamic stability analyses have been reported.[14–16] UNA monomers are according to these studies potent in decreasing or increasing base pairing specificity depending on positioning within a duplex. The comprehensive thermodynamic and spectroscopic analysis made for UNA-modified RNA duplexes revealed that stacking of nucleobases of a UNA monomer is less favorable than of RNA monomers, that overall A-form of duplexes is preserved, that UNA pyrimidine nucleotides destabilize duplexes more than UNA purine nucleotides, and that the destabilizing properties of UNA nucleotides are slightly dependent on the nature of the flanking bases.[16] Moreover, it was shown that UNA-modified antisense oligonucleotides are compatible with RNase H activity[17,18] and are highly potent in gene silencing due to increased specificity of action of siRNA duplexes.[19–23]

The 2′-*C*-piperazino-UNA-U monomer is a UNA derivative which possesses an additional positively charged piperazino moiety (Fig. 2b). It was suggested that this derivative destabilizes DNA and DNA/RNA duplexes less than regular UNA monomers and with retained mismatch discrimination.[15]

The influence of single substitution of DNA monomers of TBA with UNA monomers on thermodynamic stability, binding affinity, and biological activity of the quadruplex forming aptamer was recently reported.[24] It was shown that UNA monomers can be applied to modulate quadruplex thermodynamic stability in a position-depending manner. UNA introduced at positions U3, U7 or U12 (Fig. 1) makes quadruplex folding more energetically favorable in reference to the parent TBA with retained antiparallel, intramolecular quadruplex topology. Biological studies revealed that most of the UNA-modified TBAs possess anticoagulant properties, and that introduction of a UNA-U monomer in position 7 improves inhibition of fibrin-clot formation relative to the unmodified TBA reference aptamer.

Herein we describe thermodynamic, kinetic and biological characterization of TBA variants modified with UNA monomers in more than one position. Moreover we report chemical synthesis of a 2′-*C*-piperazino-UNA-U monomer, its introduction into specific positions of TBA, and the influence of the above modifications on thermodynamic stability, binding affinity and biological activity of the aptamer.

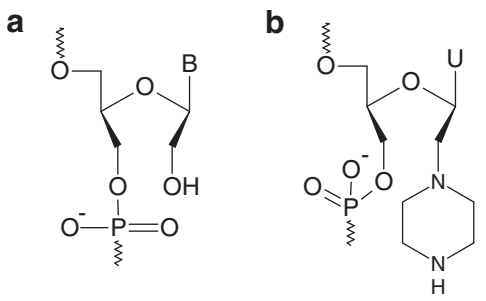

Figure 2. Structures of UNA (a) and 2′-*C*-piperazino-UNA-U (b) monomers; B = nucleobase; U = uracil-1-yl.

2. Materials and methods

2.1. Oligonucleotides

The 5′-biotinylated UNA oligonucleotides[†] (Table 1) were synthesized on an automated RNA/DNA synthesizer using standard phosphoramidite chemistry. The biotin phosphoramidite and O3′-phosphoramidites of UNA nucleotides were applied according to the previously described procedures[14] together with commercial DNA phosphoramidites. The purity of all oligonucleotides was verified by ion-exchange HPLC and determined to be 80% or greater, and the oligonucleotide compositions were confirmed by MALDI-TOF mass spectrometry (Supplementary data).

2.2. UV melting analysis of TBA variants

Oligonucleotides were dissolved in a buffer containing 100 mM KCl and 10 mM sodium cacodylate, pH 7.0. Oligonucleotide single strand concentrations were calculated using the HyTher program from the absorbance measured above 80 °C and extinction coefficients which were approximated by a nearest-neighbor model.[25,26] UNA-modified and unmodified DNA strands with identical sequences were assumed to have identical extinction coefficients. The samples were annealed for 5 min at 80 °C and then slowly cooled to room temperature. The measurements were performed for nine different concentrations of each quadruplex in the concentration range 10^{-5}–10^{-6} M using 10 mm (300 μL) quartz microcuvettes. Absorbance versus temperature curves were obtained by the UV melting method at 295 nm[27–29] in the temperature range 5–95 °C on a Beckman DU 800 spectrophotometer equipped with a six-position microcell holder and a thermoprogrammer. The reversibility of transitions was ensured for all samples by measurement of both heating and cooling profiles (data not shown). Three different heating rates (0.5 °C/min, 0.3 °C/min, and 0.2 °C/min) were tested to avoid hysteresis phenomena. The rate of 0.2 °C/min was selected because here the melting and annealing curves were reproducible and strictly superimposable. The lack of hysteresis phenomena implied that the quadruplex dissociation–association process was in a state of thermodynamic equilibrium.[27,28] Melting curves were analyzed and the thermodynamic parameters determined by non-linear curve fitting with the program MeltWin 3.5 using an unimolecular structural transition approach.[30] T_M is attributed to melting temperatures determined for the 10^{-4} M oligonucleotide concentration whereas T_m to melting points for any other concentration of an oligonucleotide.

2.3. Circular dichroism spectra

CD spectra were recorded on a Jasco J-600A spectropolarimeter using 1 mL quartz cuvettes with a 5 mm path length. The oligonucleotides were dissolved to 3.1 μM concentration in 10 mM phosphate buffered saline (138 mM NaCl, 2.7 mM KCl, 10 mM Na_2HPO_4, 1.76 mM KH_2PO_4; pH 7.4). All samples were annealed for 2 min at 100 °C and thereupon slowly cooled to room temperature before data collection. The measurements were done at 20 °C in the 200–300 nm wavelength range. The buffer spectrum was subtracted from the sample spectra. The spectra were smoothed in Microcal Origin 6.0 using a Savitzky-Golay filter.

2.4. Thermal difference spectra

The measurements were performed on a Beckman DU 800 spectrophotometer equipped with a six-position microcell holder and a

[†] UNA phosphoramidite monomers and UNA-modified oligonucleotides are commercially available from www.ribotask.dk.

Table 1
Thermodynamic parameters of DNA quadruplex formation with UNA (**U** or **G**) and 2′-*C*-piperazino-UNA-U (**X**)[a]

Name	Sequence	$-\Delta H^\circ$ (kcal/mol)	$-\Delta S^\circ$ (eu)	ΔG°_{37} kcal/mol)	T_M (°C)	$\Delta\Delta G^\circ_{37}$ (kcal/mol)	ΔT_M (°C)
TBA	GGTTGGTGTGGTTGG	36.6 ± 0.4	116.1 ± 1.3	−0.61 ± 0.02	42.2	0	0
ON1	GG**X**TGGTGTGGTTGG	36.0 ± 0.9	113.1 ± 2.8	−0.96 ± 0.03	45.4	−0.35	3.2
ON2	GGTTGG**X**GTGGTTGG	40.5 ± 0.6	127.3 ± 1.8	−1.05 ± 0.04	45.2	−0.44	3.0
ON3	GGTTGGTGTGG**X**TGG	36.6 ± 0.8	115.2 ± 2.4	−0.89 ± 0.03	44.8	−0.28	2.6
ON4	GG**U**TGGTGTGG**U**TGG	36.3 ± 0.4	113.1 ± 1.4	−1.18 ± 0.01	47.4	−0.57	5.2
ON5	GGTTGG**U**GTGG**U**TGG	38.2 ± 0.3	119.0 ± 1.0	−1.32 ± 0.01	48.1	−0.71	5.9
ON6	GG**U**TGG**U**GTGGTTGG	37.0 ± 0.3	114.6 ± 1.0	−1.50 ± 0.02	50.1	−0.89	7.9
ON7	GG**U**TGG**U**GTGG**U**TGG	37.9 ± 0.3	116.9 ± 1.0	−1.64 ± 0.02	51.0	−1.03	8.8
ON8	GGTTGG**UGU**GGTTGG	35.3 ± 2.3	117.7 ± 7.4	+1.18 ± 0.06	27.0	1.79	−15.2
ON9	GG**U**TGG**UGU**GG**U**TGG	35.8 ± 2.1	118.1 ± 7.0	+0.86 ± 0.08	29.7	1.47	−12.5

[a] Buffer: 100 mM KCl, 10 mM sodium cacodylate, pH 7.0.

thermoprogrammer using 10 mm quartz microcuvettes. The oligonucleotides were dissolved to 3.1 μM concentration in a buffer containing 100 mM KCl and 10 mM sodium cacodylate, pH 7.0. Absorbance spectra were recorded at 13 °C and 85 °C in the 220–320 nm wavelength range. The scan speed was 1200 nm/min with data collection of 1 pt/nm. Thermal difference spectra were obtained by subtraction by the low temperature absorbance spectra from the high temperature absorbance spectra with the Origin 6.0 program. The difference spectra were normalized by dividing the data by its maximum value.[31]

2.5. Isothermal titration calorimetry

The binding affinity between thrombin and aptamer was measured by isothermal titration calorimetry (iTC200, Microcal, GE). The experiments were conducted at 37 °C by injecting 100 μM aptamer in 10 mM phosphate buffered saline (138 mM NaCl, 2.7 mM KCl, 10 mM Na_2HPO_4, 1.76 mM KH_2PO_4; pH 7.4) into a 5 μM solution of thrombin. Examples of ITC heat traces are shown in Figure 3 for the aptamers **ON1**, **ON2** and **ON3**. The heat of dilution was measured by injecting 100 μM aptamer into buffer and was subsequently subtracted in the data analysis. All ITC experiments include a single pre-injection of 0.2 μL, which was discarded from the analysis, followed by 19 × 2 μL injections. The ITC heat trace was processed by custom made software as described previously[32] and fitted to a single site binding model based on the equation: $AT \rightleftharpoons A + T$, which is governed by the equilibrium dissociation constant, K_D. The results are compiled in Table 2.

2.6. Thrombin time assay

The inhibitory effect of TBA and the UNA-modified variants on clotting time was measured by a thrombin time assay. The time (in seconds) for clotting at 37 °C was measured on a STA-R EVOLUTION instrument (Stago) after mixing the identical volumes of citrate plasma and Thrombin reagent (STA-THROMBIN 00611, Diagnostica Stago). A pool of plasma from four healthy individuals was used. The thrombin reagent was pre-incubated with TBA or the TBA variants at 0.33 mM concentration for 5 min before addition to plasma and measurement of clotting time (= thrombin time). The antithrombin effect is the additional time for clotting in presence of the aptamers relative to a reference with water added.

2.7. Chemical synthesis of the uracil derivative of 2′-*C*-piperazino-UNA

All reagents and solvents were of analytical grade as obtained form commercial suppliers and used without further purification

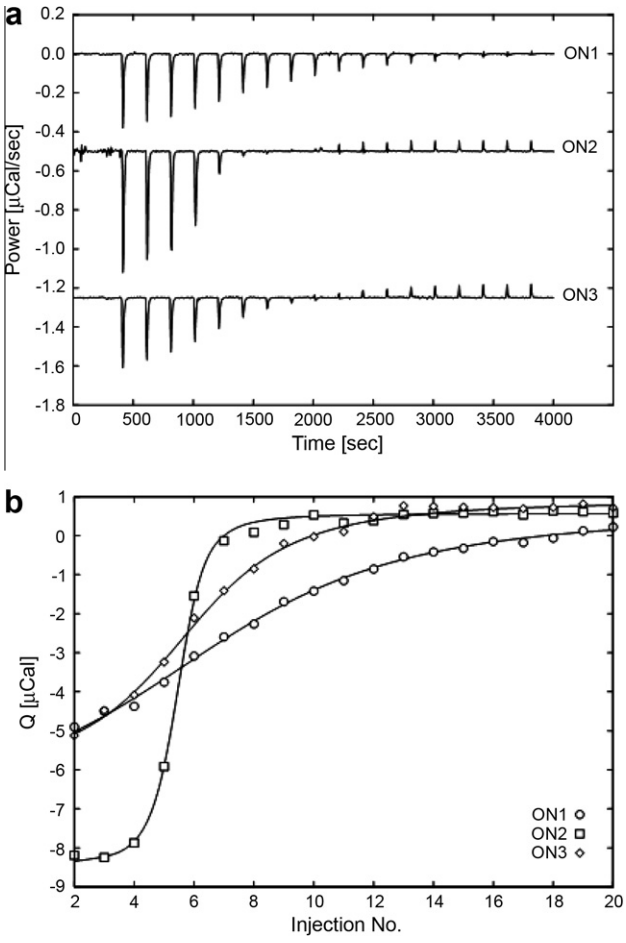

Figure 3. ITC binding affinity study of thrombin and aptamer conducted at 37 °C (a) examples of ITC heat traces of 100 μM aptamer (**ON1**, **ON2** and **ON3**) titrated into 5 μM thrombin (b) the corresponding heat of reaction. The data was analyzed using a single site binding model and the best fits are given by the solid lines in (b).

except for CH_2Cl_2 which was distilled before use. Anhydrous CH_2Cl_2 was dried over activated 4 Å molecular sieves. All reactions (Fig. 4) were monitored by thin layer chromatography (TLC) using precoated aluminum plates with indicator. Purification of the compounds was carried out by silica gel column chromatography. Afterwards, all fractions containing product were pooled, evaporated to dryness and dried under vacuum for at least 12 h. NMR spectra were recorded on a 400 MHz instrument. Chemical shifts are reported in ppm relative to TMS (^{1}H; internal standard, σ_H 0.00 ppm), solvents peaks (^{13}C, σ_C 77.0 ppm, DMSO-d_6 39.52 ppm) or 85% H_3PO_4 (^{31}P; external standard, σ_P H_3PO_4

Table 2
Binding affinity and biological effect of TBA modified TBA variants

Name[a]	K_D[b] (nM)	T-time/antithrombin effect[c] (s)
TBA	47.6	32.6/13.6
ON1	1600	21.3/2.3
ON2	52.6	31.2/12.2
ON3	1000	22.5/3.5
ON4	n.d.	19.4/0.4
ON5	300	28.7/9.7
ON6	1300	31.2/12.2
ON7	n.d.	19.5/0.5
ON8	1500	20.5/1.5
ON9	n.d.	19.0/0.0

[a] 5′-Biotinylated oligonucleotides.
[b] The relative errors for K_D values are below 27%, K_D value for 5′GGTTGG**U**GTGGTTGG is 37.0 nM.
[c] 'T-time' is the time required for a clot formation in the plasma from a blood sample; 'Antithrombin effect' is the T-time in the presence of an aptamer minus the T-time in the absence of an aptamer; no oligo added resulted in 18.9 and 19.0 s clotting times in two experimental sets and constitute reference values in the antithrombin effect calculations. Non-biotin conjugated TBA results in 34.4 s clotting time.
n.d. stands for not determined.

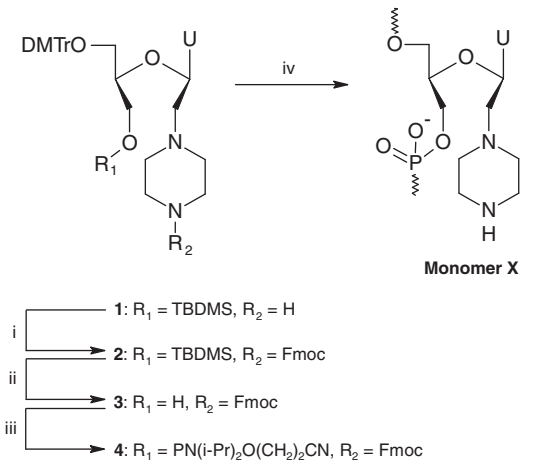

Figure 4. Chemical synthesis of 2′-*C*-piperazino-UNA-U monomer (Monomer **X**). Reagents and conditions: (i) Fmoc-Cl, anhyd CH_2Cl_2:pyridine (4:1), rt, 2.5 h (89%); (ii) triethylamine trihydrofluoride, pyridinium hydrochloride, anhyd THF, rt, 4 h, (83%); (iii) diisopropylammonium tetrazolide, 2-cyanoethyl *N*,*N*,*N*′,*N*′-tetraisopropylphosphorodiamidite, anhyd CH_2Cl_2, rt, 17 h (91%).

0.00 ppm). Assignments of NMR signals are based on 2D correlation experiments. High-resolution mass spectra (ESI-HRMS) were recorded on a mass spectrometer in positive ion mode.

2.7.1. 3′-*O*-*tert*-Butyldimethylsilyl-2′-deoxy-5′-*O*-(4,4′-dimethoxytrityl)-2′-(4-(9-fluorenylmethoxycarbonyl)piperazino)-2′,3′-secouridine (2)

Nucleoside **1**[33] (402 mg, 0.550 mmol) was dissolved in a 4:1 solution of anhyd CH_2Cl_2 and anhyd pyridine (20 mL) and the resulting mixture was cooled to 0 °C and stirred under an atmosphere of argon. 9-Fluorenylmethyl chloroformate (FmocCl, 171 mg, 0.660 mmol) was added to the reaction mixture and stirring was continued for 2 h. EtOH (1 mL) was added and the reaction mixture was stirred for additional 10 min. The solvent was removed by evaporation under reduced pressure. The afforded residue was redissolved in EtOAc (100 mL). The solution was washed with satd aq $NaHCO_3$ (2 × 50 mL). The organic phase was dried (Na_2SO_4), filtrated and evaporated to dryness under reduced pressure. The residue was purified by silica gel column chromatography using as eluent MeOH (0–5%) in CH_2Cl_2 affording nucleoside **2** as a white solid (470 mg, 89%). ^{1}H NMR (400 MHz, DMSO) δ 11.36 (br s, 1H, NH), 7.86 (d, J = 7.5 Hz, 2H), 7.62 (m, 3H), 7.46–7.10 (m, 13H), 6.85 (m, 4H), 5.98 (t, J = 6.2 Hz, 1H, H1′), 5.53 (d, J = 8.0 Hz, 1H, H5), 4.37 (d, J = 6.4 Hz, 2H, CH_2, Fmoc), 4.25 (t, J = 6.3 Hz, 1H, CH, Fmoc), 3.73 (s, 6H, 2×OMe), 3.67–3.52 (m, 3H, H3′, H4′), 3.20 (s, 4H, piperazino), 3.05–2.90 (m, 2H, H5′), 2.81–2.55 (m, 2H, H2′), 2.45–2.21 (m, 4H, piperazino), 0.78 (s, 9H, 3×Me), −0.02 (s, 3H, Me), −0.03 (s, 3H, Me). ^{13}C NMR (101 MHz, DMSO) δ 163.10, 157.94, 154.10, 151.24, 144.68, 143.75, 142.47, 140.69, 139.32, 137.33, 135.50, 135.31, 129.45, 128.82, 127.65, 127.46, 127.18, 126.98, 126.50, 124.84, 121.28, 119.93, 113.04, 113.01, 109.64, 101.79, 85.34, 81.16, 78.22, 66.24, 63.03, 62.01, 60.15, 59.28, 54.90, 54.34, 46.69, 45.54, 43.32, 25.56, 17.68, −5.64, −5.70. Anal. for $C_{55}H_{64}N_4O_9Si\cdot 1/9\ H_2O$: C, 68.77; H, 6.80; N, 5.74 (calcd C, 69.16; H, 6,78; N, 5.87). ESI-HRMS: m/z 975.4323 ([M+Na]$^+$; $C_{55}H_{64}N_4O_9Si\cdot$Na calcd 975.4335).

2.7.2. 2′-Deoxy-5′-*O*-(4,4′-dimethoxytrityl)-2′-(4-(9-fluorenylmethoxycarbonyl)piperazino)-2′,3′-secouridine (3)

Nucleoside **2** (465 mg, 0.489 mmol) was dissolved in anhyd THF (15 mL) and stirred at rt under an atmosphere of argon. Pyridinium hydrochloride (565 mg, 4.89 mmol) and triethylamine trihydrofluoride (1.18 mL, 7.24 mmol) were added and the resulting mixture was stirred for 4 h. The reaction mixture was diluted with CH_2Cl_2 (50 mL) and washed with satd aq $NaHCO_3$ (2 × 50 mL). The organic phase was dried (Na_2SO_4), filtrated and evaporated to dryness under reduced pressure. The residue was purified by silica gel column chromatography using as eluent MeOH (0–10%) in CH_2Cl_2 affording nucleoside **3** as a white foam (351 mg, 83%). ^{1}H NMR (400 MHz, $CDCl_3$) δ 8.92 (s, 1H, NH), 7.76 (d, J = 7.5 Hz, 2H), 7.55 (d, J = 7.4 Hz, 2H), 7.44–7.16 (m, 14H), 6.81 (d, J = 8.7 Hz, 4H), 5.90 (d, J = 6.6 Hz, 1H, H1′), 5.58 (d, J = 8.0 Hz, 1H, H5), 4.97 (s, 1H, 3′-OH), 4.44 (d, J = 6.6 Hz, 2H, CH_2 Fmoc), 4.22 (t, J = 6.6 Hz, 1H, CH Fmoc), 3.78 (s, 6H, 2×OMe), 3.72–3.37 (m, 7H, H3′, H4′ and piperazino), 3.15 (d, J = 5.1 Hz, 2H, H5′), 2.56 (m, 6H, H2′ and piperazino). ^{13}C NMR (101 MHz, $CDCl_3$) δ 162.90, 158.60, 154.97, 150.15, 144.45, 143.92, 141.34, 139.30, 135.61, 135.52, 129.91, 129.89, 127.94, 127.88, 127.72, 127.08, 126.98, 124.91, 120.00, 113.18, 102.56, 86.62, 84.19, 83.38, 77.34, 77.23, 77.03, 76.71, 67.30, 63.59, 63.05, 62.68, 55.25, 53.70, 53.43, 47.33, 43.34. Anal. for $C_{49}H_{50}N_4O_9\cdot 1/2\ H_2O$: C, 69.18; H, 5.91; N, 6.45 (calcd C, 69.41; H, 6.06; N, 6.61). ESI-HRMS: m/z 861.3473 ([M+Na]$^+$; $C_{49}H_{50}N_4O_9\cdot$Na calcd 861.3470).

2.7.3. 3′-*O*-(2-Cyanoethoxy(diisopropylamino)phosphino)-2′-deoxy-5′-*O*-(4,4′-dimethoxytrityl)-2′-(4-(9-fluorenylmethoxycarbonyl)piperazino)-2′,3′-secouridine (4)

Nucleoside **3** (220 mg, 0.262 mmol) was dissolved in anhyd CH_2Cl_2 (12 mL) and the solution was stirred at rt under an atmosphere of argon. Diisopropyl ammonium tetrazolide (119 mg, 0.393 mmol) and bis(*N*,*N*-diisopropylamino)-2-cyanoethoxyphosphine (67 μL, 0.393 mmol) were added and the resulting solution was stirred for 17 h and then diluted with satd aq $NaHCO_3$ (25 mL) and extracted with CH_2Cl_2 (2 × 50 mL). The organic phase was dried (Na_2SO_4), filtrated and evaporated to dryness under reduced pressure. The afforded residue was purified by silica gel column chromatography using as eluent EtOAc (50–100%) in PE affording phosphoramidite **4** as a white foam (249 mg, 91%). ^{31}P NMR (162 MHz, $CDCl_3$) δ 148.9, 148.5. Anal. for $C_{58}H_{67}N_6O_{10}P\cdot 1/25\ H_2O$: C, 66.60; H, 6.55; N, 7.75 (calcd C, 66.99; H, 6.50; N, 8.08). ESI-HRMS: m/z 1061.4528 ([M+Na]$^+$, $C_{58}H_{67}N_6O_{10}P\cdot$Na calcd 1061.4548).

3. Results

3.1. Chemical synthesis of 2′-*C*-piperazino UNA uridine

The starting material (Fig. 4, compound **1**) was prepared as earlier described.[33] Protection of the piperazino moiety was carried out

with Fmoc-Cl in anhyd CH_2Cl_2/pyridine (4:1) affording compound **2** in 89% yield. Desilylation using triethyl trihyrdofluoride and pyridinium hydrochloride in THF (giving compound **3**, 85% yield) followed by O3′-phosphitylation by reaction with 2-cyanoethyl *N*,*N*,*N*′,*N*′-tetraisopropylphosphorodiamidite and diisopropylammonium tetrazolide in CH_2Cl_2 afforded phosphoramidite **4** in 91% yield suitable for incorporation of monomer **X** into ONs on an automated DNA synthesizer (**ON1**–**ON3**, Table 1). This was carried out using 1H-tetrazole as activator and 10 min coupling time. The stepwise coupling yields for amidite **4** was ~97% whereas the unmodified DNA amidites displayed >97% coupling yield (2 min coupling time).

3.2. Thermodynamic and structural features

UNA and 2′-*C*-piperazino-UNA residues were placed in specific positions of TBA which were previously reported as stabilizing for quadruplex structure upon single introduction of UNA monomers (Table 1, **ON1**–**ON7**).[24] The influence of radically increased flexibility of quadruplex structure was furthermore tested for two variants with an entirely UNA-modified central loop (**ON8**, **ON9**). Most of variants studied herein were found as more stable in reference to unmodified TBA. A single introduction of the 2′-*C*-piperazino-UNA monomer in positions U3, U7 or U12 enhanced the thermodynamic stability of the quadruplex structure by 0.28–0.44 kcal/mol. Two or three UNA residues placed in various combinations in positions U3, U7, and U12 increased thermodynamic stability by 0.57–1.03 kcal/mol. Conversely, significant destabilization mounting to 1.79 kcal/mol was observed for variants with an entirely UNA-modified central loop. The T_m values found for each of the variants were concentration independent (data not shown).

Circular dichroism (CD) and thermal difference (TDS) spectra were recorded to evaluate possible changes in quadruplex conformation and topology (Figs. 5 and 6). All thermodynamically stable variants (**ON1**–**ON7**) show patterns similar to that of unmodified TBA. CD spectra of **ON1**–**ON7** were characterized by high-amplitude, positive maxima at 293 nm with increased intensity in reference to TBA. The TDS patterns with two positive maxima near 240 and 270 nm, a moderately intense peak around 260 nm, and an intense peak around 295 nm, were identical with that of the unmodified aptamer. In contrast, unstable **ON8** and **ON9** showed CD bands of strongly decreased intensity and TDS signatures untypical for a quadruplex structure.

3.3. Thrombin binding affinity of aptamers

Isothermal titration calorimetry (ITC) was applied to determine the thrombin binding affinity of the modified TBA variants (Table 2). Only variant **ON2** showed comparable binding relative to unmodified TBA. Variants **ON1**, **ON3**, **ON5**, **ON6**, and **ON8** showed significantly decreased affinity to thrombin, whereas the K_D value for three remaining variants (**ON4**, **ON7**, and **ON9**) could not be determined due to very low binding affinity.

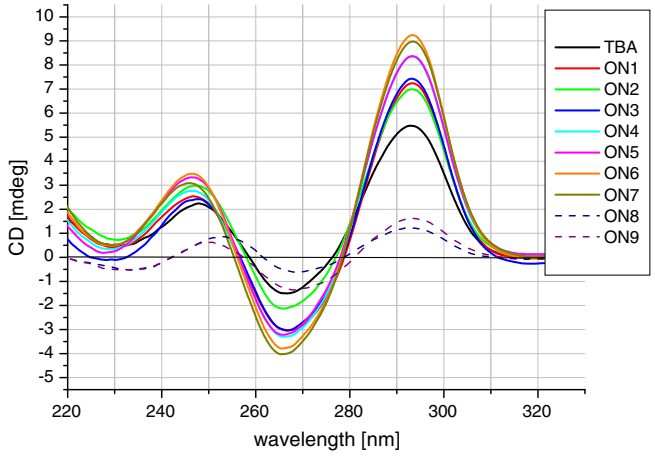

Figure 5. CD spectra of TBA and modified variants.

3.4. Biological studies

The influence of modified TBA variants on enzymatic activity of thrombin was investigated using a thrombin time assay (Table 2). Three variants, namely **ON2**, **ON5**, and **ON6** showed inhibitory effects slightly weaker but comparable to unmodified TBA. Significantly reduced inhibition of fibrin-clot formation was observed for aptamers **ON1**, **ON3**, **ON8**, whereas **ON4**, **ON7**, and **ON9** were shown not to have any significant impact on the coagulation process.

4. Discussion

Thermodynamic investigation of the stability of singly UNA-modified TBA variants was recently described and three positions (U3, U7, and U12) were found as energetically favorable for UNA introduction.[24] Substitution of the above three positions with the 2′-*C*-piperazino-UNA uridine monomer **X** results in further increase of quadruplex thermodynamic stability (Table 1). Monomer **X** decreases quadruplex free energy by 0.35, 0.44, and 0.28 kcal/mol (**ON1**, **ON2** and **ON3**, respectively) what corresponds to approximate 2-fold more favorable equilibrium constant for quadruplex formation relative to that of the TBA reference. It was previously reported that a single UNA-U monomer stabilizes the TBA structure by 0.23 (U3), 0.50 (U7) and 0.15 (U12) kcal/mol.[24] The energetically favorable change of Gibbs′ free energy ($\Delta\Delta G^{\circ}_{37}$) observed for variants **ON1** and **ON3** is therefore attributed not only to the presence of the flexible UNA monomer but also to the presence of the piperazino moiety. Similar behavior has been reported previously for DNA/DNA and DNA/RNA duplexes modified with the 2′-*C*-piperazino-UNA monomer.[15] The increased stabilization of duplexes modified with 2′-*C*-piperazino-UNA monomer in reference to those containing UNA monomer was ascribed to partial neutralization of the negatively charged backbone by the positively charged piperazino moiety. Hence, analogous electrostatic effects might be responsible for the additional stabilization of quadruplex structure observed for variants modified with the 2′-*C*-piperazino-UNA uridine monomer.

The introduction of two or three UNA-U monomers in more than one of the specific positions found previously as energetically favorable resulted in all cases in an increase of quadruplex thermodynamic stability (**ON4**–**ON7**). Notably, the energetic gain resulting from the presence of two or three UNA-U residues is additive, although even slightly higher than the sum of single substitution effects.[24] Accordingly, the highest thermodynamic stability was achieved by incorporation of three UNA-U monomers in positions U3, U7 and U12 (**ON7**, Table 1) leading to a decrease of Gibbs′ free energy by about 1 kcal/mol. Such improvement can be translated to a 5-fold more favorable equilibrium constant for quadruplex formation in reference to that of unmodified TBA.

Significantly increased flexibility of the middle loop was achieved by substituting all three loop residues for UNA monomers (**ON8**, Table 1). This resulted in significant destabilization of the quadruplex structure by 1.79 kcal/mol corresponding to an 18-fold more unfavorable equilibrium constant for quadruplex formation in reference to that of TBA. The positive value of Gibbs′ free energy for **ON8** indicates that under the conditions used herein the predominant species is the unfolded form. Additional introduction of UNA monomers in positions U3 and U12 (**ON9**) increases quadruplex stability by 0.32 kcal/mol in reference to **ON8**, which is in

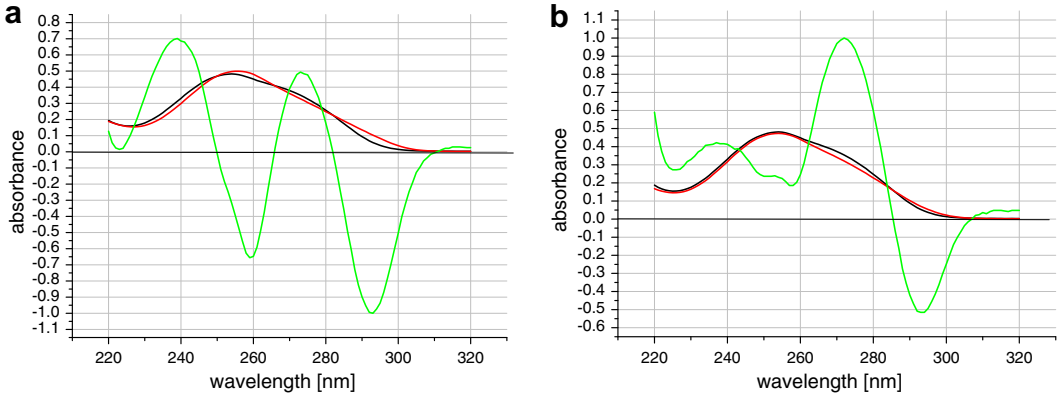

Figure 6. Thermal difference spectra (green) of (a) **ON1** (characteristic also for TBA, **ON2-ON7**) and (b) **ON8** (characteristic also for **ON9**). High- and low-temperature spectra are marked in black and red, respectively.

agreement with the previously reported thermodynamic effect of UNA-U placed in positions U3 and U12.[24] The overall stability of **ON9** is however reduced (a 10-fold decrease in the equilibrium constant for quadruplex formation) relative to that of unmodified TBA.

The molecularity of folding of all variants studied herein was verified by monitoring the concentration dependence of T_m values[29] to be intramolecular as all studied quadruplexes revealed no linear increase in the function of T_m versus aptamers concentration (data not shown). The results confirm a previous report showing that UNA monomers do not impact the folding molecularity of TBA.[24]

Quadruplexes posses various folding topologies which can be easily distinguished by different CD profiles.[34] CD spectra for all thermodynamically stable variants (TBA and **ON1**–**ON7**) show a high-amplitude band near 293 nm characteristic for an antiparallel folding topology (Fig. 5). Moreover, the intensity of the band in CD profiles of **ON1**–**ON7** is increased in reference to that of unmodified TBA. Two modified aptamers with positive ΔG°_{37} value (**ON8** and **ON9**) show significant decrease of characteristic bands intensity suggesting a disruption of quadruplex structure. TDS profiles support the results obtained from CD measurements. The TDS shapes of TBA and **ON1**–**ON7** are specific for intramolecular quadruplex structures with two maxima at 240 and 273 nm and two minima at 260 and 295 nm (Fig. 6).[31] The irregular TDS profiles observed for **ON8** and **ON9** indicate more unstructured states for these constructs.[24]

The isothermal titration calorimetry studies revealed that only the aptamer modified with 2′-*C*-piperazino-UNA-U monomer (**X**) in position 7 posses comparable thrombin binding affinity as unmodified TBA (**ON2**, Table 2). X-ray studies of a TBA-thrombin complex revealed that T7 is plunged into a hydrophobic cluster within the fibrinogen recognition exosite.[11,12] Moreover, it was suggested that a UNA-U monomer introduced in position U7 induces favorable structural changes and in consequence improves aptamer affinity towards thrombin (K_D determination using surface plasmon resonance (SPR)).[24] ITC studies show similar trend for K_D change of UNA-modified aptamer in position 7 (variant U7, Table 2). Slightly worse affinity of **ON2** towards thrombin in reference to TBA and variant U7 suggests that the presence of the positively charged 2′-*C*-piperazino-UNA-U monomer is decreasing thrombin affinity. The two remaining aptamers modified by 2′-*C*-piperazino-UNA-U in position 3 or 12 (**ON1** and **ON3**, respectively) show more than 20-fold higher K_D value, whereas their UNA-modified counterparts showed only moderate changes in reference to that of TBA (less than 2-fold change of K_D)[24] what confirms an unfavorable impact of the piperazino moiety on the interaction with thrombin. The negative influence of piperazino moiety on aptamers binding affinity might originate from the presence of the positively charged piperazino moiety interacting electrostatically with the positively charged protein, but possibly also from steric hindrance. According to NMR studies, T3 and T12 are situated in close proximity to the thrombin anion exosite I,[7,12] wherefore the presence of the bulky piperazino moiety might inhibit an optimal fit between aptamer and thrombin.

It was suggested that high stability of quadruplex structure is essential for proper and specific interactions between aptamer and thrombin.[35] The results described herein reveal that the most thermodynamically stable aptamer **ON7** is a very poor binder (Table 2, K_D not determined) as is **ON9**. Notably, the latter display a positive Gibbs′ free energy (**ON9**) upon denaturation indicating predominance of unfolded states. Similarly, also **ON4**, **ON6**, and **ON8** posses at least 27-fold decreased binding affinity towards thrombin in reference to TBA. Moreover, moderate binding affinity decreased by about 6-fold in reference to TBA was found for **ON5** which is characterized by improved thermodynamic stability. The significantly reduced binding affinity towards thrombin for the majority of variants studied herein suggests that thermodynamic stability of quadruplexes, or even predominant quadruplex structure, is not the excusive determinant of specific interactions between aptamer and thrombin.

The thrombin time assay partially confirmed results derived from ITC studies. Biological activity of most of the studied variants (**ON1**, **ON3**, **ON4**, **ON7**, **ON8**, and **ON9**, Table 2) which posses poor thrombin binding affinity was significantly decreased in reference to that of unmodified TBA. In contrast, **ON5** characterized by only a moderate K_D value shows considerable ability to inhibit fibrin clot formation. Surprisingly **ON6** seems to have biological activity comparable to that of TBA despite strongly decreased binding affinity towards thrombin. However, incorporation of 2′-*C*-piperazino-UNA-U monomer **X** at position 7 of the aptamer results not only in improved thermodynamic stability and a K_D value similar to that of TBA, but also in inhibition of fibrin clotting as for TBA.

5. Conclusions

The results described herein confirm that UNA monomers are suitable tools to achieve extraordinarily stabilized quadruplexes. Additional functionalization of the UNA-U monomer by a piperazino moiety decreases free energy of quadruplex formation even further. The presence of 2′-*C*-piperazino-UNA monomer or several UNA monomers within the aptamer has a negative effect on binding affinity and biological activity for the majority of studied

variants. Nevertheless, one of the aptamers, modified by the 2′-*C*-piperazino-UNA-U monomer at position 7, possess improved thermodynamic stability and binding affinity and inhibitory properties comparable to those of unmodified TBA. Our results provide insights into specific interactions between TBA and thrombin and constitute a new alternative of improving the thermodynamic stability of quadruplexes.

Acknowledgments

The Nucleic Acid Center is a research center of excellence funded by The Danish National Research Foundation for studies on nucleic acid chemical biology. We gratefully acknowledge financial support by The Danish National Research Foundation.

Supplementary data

Supplementary data associated with this article can be found, in the online version, at doi:10.1016/j.bmc.2011.06.087.

References and notes

1. Walker, C. P. R.; Royston, D. *Br. J. Anaesth.* **2002**, *88*, 848.
2. Agnelli, G.; Sonaglia, F.; Becattini, C. *Curr. Pharm. Des.* **2005**, *11*, 3885.
3. Kuderer, N. M.; Khorana, A. A.; Lyman, G. H.; Francis, C. W. *Cancer* **2007**, *110*, 1149.
4. Lettino, M.; Toschi, V. *Curr. Med. Chem. Cardiovasc. Hematol. Agents* **2004**, *2*, 267.
5. G. T. Gerotziafasa, C. Papageorgiouc, M. Hatmid, M. M. Samamad, and I. Elalamya, *Pathophysiol. Haemos. Thromb.*, 2007/2008, **36**, 204.
6. Bock, L. C.; Griffin, L. C.; Latham, J. A.; Vermaas, E. H.; Toole, J. J. *Nature* **1992**, *355*, 564.
7. Kelly, J. A.; Feigon, J.; Yeates, T. O. *J. Mol. Biol.* **1996**, *256*, 417.
8. Macaya, R. F.; Schultze, P.; Smith, F. W.; Roe, J. A.; Feigon, J. *Proc. Nat. Acad. Sci. U.S.A.* **1993**, *90*, 3745.
9. Lancellotti, S.; De Cristofaro, R. *Cardiovasc. Hematol. Agents Med. Chem.* **2009**, *7*, 19.
10. Khati, M. *J. Clin. Pathol.* **2010**, *63*, 480.
11. Padmanabhan, K.; Padmanabhan, K. P.; Ferrara, J. D.; Sadler, J. E.; Tulinsky, A. *J. Biol. Chem.* **1993**, *268*, 17651.
12. Padmanabhan, K.; Tulinsky, A. *Acta Crystallogr. Sect. D* **1996**, *D52*, 272.
13. Nielsen, P.; Dreiøe, L. H.; Wengel, J. *Bioorg. Med. Chem. Lett.* **1995**, *3*, 19.
14. Langkjær, N.; Pasternak, A.; Wengel, J. *Bioorg. Med. Chem.* **2009**, *17*, 5420.
15. Jensen, T. B.; Langkjær, N.; Wengel, J. *Nucleic Acids Symp. Ser.* **2008**, *52*, 133.
16. Pasternak, A.; Wengel, J. *Nucleic Acids Res.* **2010**, *38*, 6697.
17. Mangos, M. M.; Min, K.-L.; Viazovkina, E.; Galarneau, A.; Elzagheid, M. I.; Parniak, M. A.; Damha, M. J. *J. Am. Chem. Soc.* **2002**, *125*, 654.
18. Fluiter, K.; Mook, O. R. F.; Vreijling, J.; Langkjær, N.; Højland, T.; Wengel, J.; Baas, F. *Mol.Biosyst.* **2009**, *5*, 838.
19. Pasternak, A.; Wengel, J. *Org. Biomol. Chem.* **2011**, *9*, 3591.
20. Bramsen, J. B.; Laursen, M. B.; Nielsen, A. F.; Hansen, T. B.; Bus, C.; Langkjær, N.; Babu, B. R.; Højland, T.; Abramov, M.; Van Aerschot, A.; Odadzic, D.; Smicius, R.; Haas, J.; Andree, C.; Barman, J.; Wenska, M.; Srivastava, P.; Zhou, C.; Honcharenko, D.; Hess, S.; Muller, E.; Bobkov, G. V.; Mikhailov, S. N.; Fava, E.; Meyer, T. F.; Chattopadhyaya, J.; Zerial, M.; Engels, J. W.; Herdewijn, P.; Wengel, J.; Kjems, J. *Nucleic Acids Res.* **2009**, *37*, 2867.
21. Bramsen, J. B.; Pakula, M. M.; Hansen, T. B.; Bus, C.; Langkjær, N.; Odadzic, D.; Smicius, R.; Wengel, S. L.; Chattopadhyaya, J.; Engels, J. W.; Herdewijn, P.; Wengel, J.; Kjems, J. *Nucleic Acids Res.* **2010**, *38*, 5761.
22. Kenski, D. M.; Cooper, A. J.; Li, J. J.; Willingham, A. T.; Haringsma, H. J.; Young, T. A.; Kuklin, N. A.; Jones, J. J.; Cancilla, M. T.; McMasters, D. R.; Mathur, M.; Sachs, A. B.; Flanagan, W. M. *Nucleic Acids Res.* **2010**, *38*, 660.
23. Vaish, N.; Chen, F.; Seth, S.; Fosnaugh, K.; Liu, Y.; Adami, R.; Brown, T.; Chen, Y.; Harvie, P.; Johns, R.; Severson, G.; Granger, B.; Charmley, P.; Houston, M.; Templin, M. V.; Polisky, B. *Nucleic Acids Res.* **2011**, *39*, 1823.
24. Pasternak, A.; Hernandez, F. J.; Rasmussen, L. M.; Vester, B.; Wengel, J. *Nucleic Acids Res.* **2011**, *39*, 1155.
25. Borer, P. N. In *Optical properties of nucleic acids, absorption and circular dichroism spectra*; Fasman, G. D., Ed.; Cleveland: OH, 1975.
26. Richards, E. G. In *Use of tables in calculations of absorption, optical rotatory dispersion and circular dichroism of polyribonucleotides*; Fasman, G. D., Ed.; Cleveland: OH, 1975.
27. Rachwal, P. A.; Fox, K. R. *Methods* **2007**, *43*, 291.
28. Mergny, J.-L.; Lacroix, L. *Curr. Protocols Nucleic Acid Chem.* **2009**, *17*, 1.1.
29. Mergny, J.-L.; Lacroix, L. *Oligonucleotides* **2003**, *13*, 515.
30. McDowell, J. A.; Turner, D. H. *Biochemistry* **1996**, *35*, 14077.
31. Mergny, J.-L.; Li, J.; Lacroix, L.; Amrane, S.; Chaires, J. B. *Nucleic Acids Res.* **2005**, *33*, e138.
32. Henriksen, J. R.; Andresen, T. L.; Feldborg, L. N.; Duelund, L.; Ipsen, J. H. *Biophys. J.* **2010**, *98*, 2199.
33. Karlsen, K. K.; Jensen, T. B.; Wengel, J. *J. Org. Chem.* **2009**, *74*, 8838.
34. Tang, C.-F.; Shafer, R. H. *J. Am. Chem. Soc.* **2006**, *128*, 5966.
35. Paborsky, L. R.; McCurdy, S. N.; Griffin, L. C.; Toole, J. J.; Leung, L. L. *J. Biol. Chem.* **1993**, *268*, 20808.